Four-dimensional isotopic approach to identify perchlorate sources in groundwater: Application to the Rialto-Colton and Chino subbasins, southern California (USA)

Paul B. Hatzinger[a,*], J.K. Böhlke[b], Neil C. Sturchio[c], John Izbicki[d], Nicholas Teague[d]

[a] *Aptim Federal Services, Lawrenceville, NJ, USA*
[b] *U.S. Geological Survey, Reston, VA, USA*
[c] *University of Delaware, Newark, DE, USA*
[d] *U.S. Geological Survey, San Diego, CA, USA*

ARTICLE INFO

ABSTRACT

Perchlorate (ClO_4^-) in groundwater can be from synthetic or natural sources. Natural sources include ClO_4^- associated with historical application of imported natural nitrate fertilizer from the Atacama Desert of Chile, and indigenous ClO_4^- that accumulates locally in arid regions from atmospheric deposition. The Rialto-Colton groundwater subbasin, 80 km east of Los Angeles, California, includes two mapped ClO_4^- plumes from known military/industrial sources. Larger areas downgradient from those plumes, and in the Chino subbasin to the southwest, also contain ClO_4^-. Perchlorate from wells was analyzed for chlorine and oxygen stable isotope ratios ($\delta^{37}Cl$, $\delta^{18}O$, $\Delta^{17}O$) and radioactive chlorine-36 (^{36}Cl) isotopic abundance, along with other geochemical, isotopic, and hydrogeologic data. Isotopic data show that synthetic ClO_4^- was the dominant source within the mapped plumes. Downgradient from the mapped plumes, and in the Chino subbasin, the dominant source of ClO_4^- was related to past agricultural use of Chilean (Atacama) nitrate fertilizer. The ^{36}Cl and $\delta^{18}O$ data indicate that wells having predominantly synthetic or Atacama ClO_4^- also contained small fractions of indigenous ClO_4^-. Little or no differences were observed in isotopic composition or ClO_4^- source with depth in depth-dependent data from selected wells. Indigenous ClO_4^- was most evident in upgradient wells having ClO_4^- concentrations < 1 μg/L, consistent with its occurrence as a background constituent throughout the region. Stable isotope ratios of chlorine and oxygen and ^{36}Cl isotopic abundance data provided relatively unambiguous discrimination of synthetic and Atacama sources in most wells having ClO_4^- concentrations greater than 1 μg/L.

1. Introduction

1.1. Background

The contamination of groundwater and drinking water by perchlorate (ClO_4^-) has become an issue of national concern because of the adverse health effects of ClO_4^- ingestion. ClO_4^- in the environment can be from synthetic or natural sources. Ammonium ClO_4^- is widely used as an oxidant in solid propellants (Cunniff et al., 2006), so it was once assumed that ClO_4^- contamination of groundwater largely resulted from historical testing and disposal practices by the military, the aerospace and ordnance industries, and ClO_4^- manufacturers. However, a variety of commercial products also contain synthetic ClO_4^- either intentionally or as a manufacturing byproduct, including fireworks, matches, air bags, road flares, perchloric acid, and chlorate

herbicides (Trumpolt et al., 2005; Aziz and Hatzinger, 2008), some of which may contribute to ClO_4^- in groundwater (Munster et al., 2008; Böhlke et al., 2009; Munster and Hanson, 2009).

Natural sources of ClO_4^- include Chilean nitrate fertilizers and indigenous ClO_4^- that appears to form atmospherically and accumulate in vadose soils in arid environments. ClO_4^- has long been known to co-occur with sodium nitrate ($NaNO_3$) in surficial deposits in the Atacama Desert of Chile at an average concentration of around 0.1% (by mass) of the total soluble salt, with concentrations as high as 6.8% reported (Schilt, 1979; Ericksen, 1981, 1983; Dasgupta et al., 2006). Processed NO_3^- deposits were widely used in the U.S. during the first half of the 20th century as a source of inorganic nitrogen fertilizer. According to the California Department of Agriculture, more than 477,000 metric tons of imported Atacama NO_3^- was used in California as fertilizer between 1923 and 1998 (California Department of Food and

---

Agriculture, 1999). The final ClO_4^- concentration of processed Atacama NO_3^- fertilizer prior to 2002 was variable, but likely ranged from 0.15 to 1.0 wt % based upon analysis of historical samples (Eldridge et al., 2000; Urbansky et al., 2001a,b; Dasgupta et al., 2006). Changes in manufacturing processes after 2002 were reported to reduce the final ClO_4^- concentration to ≤0.01% (Dasgupta et al., 2006). Thus, apart from synthetic sources, past application of Atacama NO_3^- fertilizer provides a potential source of ClO_4^- in groundwater and drinking water in the U.S.

Natural ClO_4^- that is not associated with Chilean fertilizers has also been detected in soils, groundwaters, and mineral deposits collected from arid regions in the western U.S., including groundwater underlying an area of $155,000 \, km^2$ in the Southern High Plains (SHP) of Texas and New Mexico (Jackson et al., 2004, 2005, 2006; Dasgupta et al., 2005; Rajagopalan et al., 2006) and in the Middle Rio Grande Basin (MRGB) of New Mexico (Plummer et al., 2006). This indigenous ClO_4^- is hypothesized to form in the atmosphere through photochemical reactions (Murphy and Thomson, 2000; Bao and Gu, 2004; Dasgupta et al., 2005; Kang et al., 2008; Sturchio et al., 2009) and to reach Earth's surface via precipitation or dry deposition, resulting in long-term accumulations in arid regions (Rajagopalan et al., 2006; Rao et al., 2007). When such salt accumulations become subject to large-scale irrigation, accumulated ClO_4^- can be mobilized and transported to the water table. Such agricultural mobilization is hypothesized to account for high ClO_4^- concentrations in groundwater in West Texas, which has been widely irrigated for several decades for production of cotton and other crops (Rajagopalan et al., 2006). Irrigation also may be associated with transport of ClO_4^- to groundwater from crops treated with Atacama nitrate fertilizer (Böhlke et al., 2009; Sturchio et al., 2014).

Methods have been developed over the past decade to measure the stable isotope ratios of chlorine ($^{37}Cl/^{35}Cl$) and oxygen ($^{18}O/^{16}O$, $^{17}O/^{16}O$), and the fractional abundance of the radioactive isotope ^{36}Cl in ClO_4^- (Bao and Gu, 2004; Böhlke et al., 2005, 2009, 2017; Sturchio et al., 2006, 2009, 2012b, 2014; Poghosyan et al., 2014; Hatzinger et al., 2011, 2013). These analyses have shown that the primary source types of ClO_4^- (synthetic, Atacama, U.S. indigenous) are isotopically distinguishable. Additional background information about ClO_4^- isotopic characteristics is provided in Supporting Data, Section S1 as well as in the references cited above. The primary objective of the current study was to evaluate the combined use of four independent isotopic ratio measurements (four-dimensional isotope approach) for apportioning groundwater ClO_4^- sources in an area of southern California having complex hydrogeology and land use history, with at least three different types of potential natural and anthropogenic ClO_4^- inputs distributed heterogeneously. This study included depth-dependent sampling in some wells, along with multiple tests of sampling and analytical procedures.

1.2. Description of the study area

The study area includes the Rialto-Colton and Chino, CA subbasins of the upper Santa Ana River groundwater basin in southern California (Fig. 1) as described in detail by Izbicki et al. (2015). The study area is underlain by highly-permeable, unconsolidated alluvial-fan deposits (mainly sand and gravel) of Quaternary age between about 100 m to 240 m thick that overlie low-permeability, partly-consolidated Tertiary sediments and granitic basement (Woolfenden and Kadhim, 1997).

The Rialto-Colton subbasin is bounded by the San Jacinto and Rialto-Colton Faults (Fig. 1) that are part of the regionally active San Andreas fault system (Dutcher and Garrett, 1963). The faults are barriers to groundwater flow along most of their extent, and prior to groundwater development water level difference across the northern part of the Rialto-Colton Fault between the Rialto-Colton and Chino subbasins were as much as 120 m (Dutcher and Garrett, 1963). The Rialto-Colton subbasin contains a regional aquifer that is pumped for

water supply. Depth to water in the regional aquifer in the northern part of the subbasin can exceed 160 m. In the north, the regional aquifer is overlain by a perched aquifer about 100 m below land surface. Prior to development, groundwater recharge was from 1) local precipitation, 2) groundwater underflow across the northern part of the San Jacinto Fault that originated as infiltration from streams that drain higher elevations in the San Gabriel Mountains to the north, and 3) mountain-block recharge from the San Gabriel Mountains. As a result of development, groundwater recharge from irrigation and septic return, stormflow detention basins, and artificial recharge from northern California increased. Groundwater movement in the Rialto-Colton subbasin is from recharge areas in the north to the southeast between the San Jacinto and Rialto-Colton faults, but deviations can occur locally. The perched aquifer is not present in the southern part of the subbasin. Under predevelopment conditions, discharge from the Rialto-Colton subbasin occurred as groundwater flow toward the Santa Ana River and across the southeastern part of the Rialto-Colton Fault. As a result of development, groundwater pumping from wells is a major component of discharge from the regional aquifer.

Release of synthetic ClO_4^- from military and industrial sources in the northern part of the Rialto-Colton subbasin of San Bernardino County, CA has contaminated parts of the perched aquifer and affected a number of production wells completed in the regional aquifer. Previously identified ClO_4^- sources include: (1) a 160-acre industrial site formerly occupied by several different industries, and also known as the *Rockets, Fireworks, and Flares* (RFF) site (USEPA, 2014), and (2) properties adjacent to the current Mid-Valley Sanitary Landfill (MVSL) operated by San Bernardino County, including the Rialto Ammunition Backup Storage Point, a site of several World War II era bunkers that were later used for the manufacture, transport, and/or disposal of fireworks, flares, explosives and other potentially hazardous materials (SAIC, 2004). This site is known as the *Mid Valley Sanitary Landfill/ Bunker Site* (MSVL/Bunker Site) (GeoLogic Associates, 2003; SARWQCB, 2005; Woolfenden, 2007) or the *Former Bunker Area*. The distribution of ClO_4^- concentrations in wells indicates two parallel plumes emanating from those sites (Fig. 1). As defined by previous studies, the mapped plume from the RFF Site is parallel to the Rialto-Colton fault and extends at least 6 km downgradient of the site in the southeast direction of groundwater flow (GeoLogic Associates, 2013). Recent USEPA reports suggest that this plume may reach as far as 9 km downgradient, but the distal extent is not yet known (USEPA, 2014). The mapped plume from the MSVL/Bunker Site extends ~3 km downgradient, parallel to the RFF Site plume.

The extent of high-level ClO_4^- contamination (e.g., $> 50 \, \mu g/L$) emanating as plumes from the two military/industrial sites is reasonably well defined. However, ClO_4^- has also been detected in groundwater wells throughout the Study Area at lower concentrations (~1–20 μg/L). Perchlorate has been measured in groundwater wells to the southeast of the two known plumes in the general direction of groundwater flow, such as Colton 15 and 13B1-5 (RHSW-5), and in wells to the south of the sources but outside the hypothesized groundwater flow path, including a number of wells positioned to the south of the Rialto-Colton Fault in the Chino subbasin, such as F-4A, F-17B, F-35A, and others (Fig. 1). Several wells in the Chino subbasin positioned between the Rialto-Colton Fault and the postulated Rialto-Colton Fault West (Paulinski, 2012), such as F-26A and Chino 2 (Fig. 1), also have measurable ClO_4^-, albeit at low concentrations ($< 2 \, \mu g/L$). The general pattern of low-level ClO_4^- contamination in groundwater throughout the Study Area (apart from the plumes emanating from the two source areas) suggests the possibility of additional sources of ClO_4^- in the area, possibly including ClO_4^- derived from historical Atacama fertilizer application, indigenous natural ClO_4^-, and synthetic ClO_4^- from local uses of flares, fireworks, blasting, or other sources.
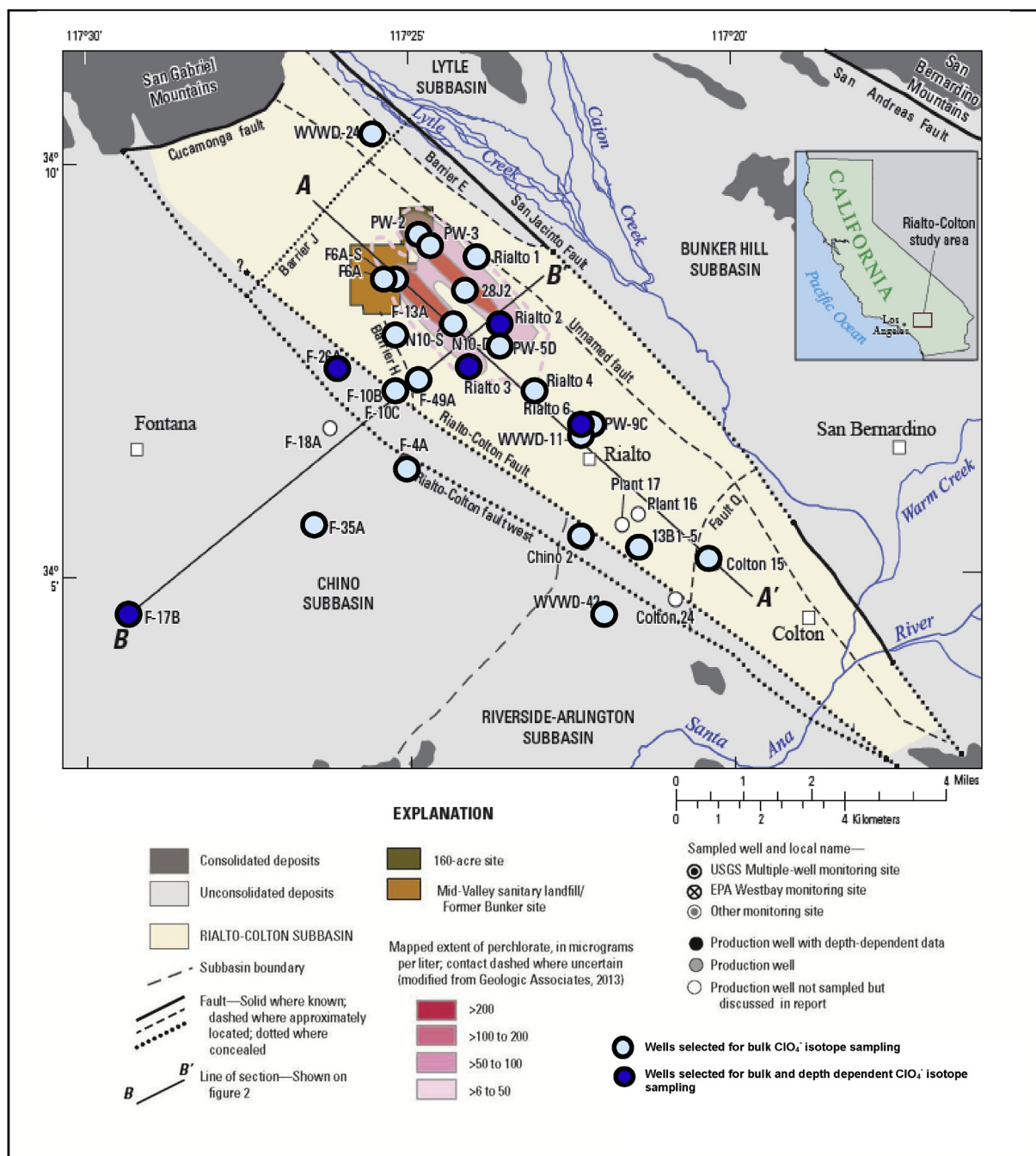
Fig. 1. Map view of the Study Area with two previously identified ClO_4^- source areas and associated groundwater perchlorate plumes delineated. Wells selected for bulk discharge ClO_4^- isotope sampling (light blue symbols) and depth-dependent ClO_4^- isotope sampling (dark blue symbols) are indicated. The plume map was generated previously and modified from GeoLogic Associates (2013) and Izbicki et al. (2015). The map does not include concentration data from the current study, or the most recent USEPA site sampling (USEPA, 2014). (For interpretation of the references to colour in this figure legend, the reader is referred to the Web version of this article.)

2. Materials and methods

2.1. Sample collection

A total of 27 wells (17 production wells, 8 monitoring wells, and 2 WestBay wells) were sampled for ClO_4^- isotopic analysis (Fig. 1). In conjunction with coupled well bore-flow and depth-dependent water quality sampling (Izbicki et al., 2015), depth-dependent ClO_4^- stable isotope samples were collected from five of the production wells. Groundwater was obtained from the 27 wells as described in Izbicki et al. (2015). In order to collect adequate quantities of ClO_4^- for

isotopic analysis, water from 25 of the wells (WestBay wells excluded) was passed through 3.2-cm inner diameter x 15.2-cm length PVC columns containing about 100 mL (∼60 g dry wt) of Purolite A-530E bifunctional anion exchange resin (IX resin), which is highly selective for ClO_4^- (Gu et al., 2007). The flow to the columns was generally set at ≤ 2.5 L per minute. Samples were periodically collected from the influent and effluent of the columns to evaluate stability of influent concentration with time, to detect column breakthrough of ClO_4^-, and to estimate the total amount of ClO_4^- trapped on each column. After a pre-determined time, ranging from a few hours to several days (based on flow rate and starting ClO_4^- concentration in each well), the IX

Table 1

Perchlorate concentrations and Cl and O isotope data for samples collected from wells in the Study Area. Perchlorate concentration data were published previously in Izbicki et al. (2015).

State well number	Local well name	$\delta^{37}Cl$ (‰)	$\delta^{18}O$ (‰)	$\delta^{17}O$ (‰)	$\Delta^{17}O$ (‰)	^{36}Cl $^{36}Cl/Cl$ x 10^{-15}	Perchlorate (µg/L) single	Perchlorate (µg/L) column influent
Wells in the perched aquifer in the Rialto-Colton subbasin within the mapped plume								
1N/5W-28J2	28J-2	0.8 ± 0.1	−18.3 ± 0.1	−9.7 ± 0.1	−0.1 ± 0.0	102 ± 1	285	261 ± 5
1N/5W-29H1	F6	−0.5	−13.5	−7.0	0.1	1040 (20)	8.8	12 ± 2
1N/5W-29H3	F6A-S	−0.9	−15.5 ± 0.3	−8.0 ± 0.0	0.2 ± 0.1	NA	0.7	1.1 ± 0.4
1N/5W-33B2	N-10S	1.0 ± 0.0	−12.5 ± 1.7	−6.6 ± 1.0	0.0 ± 0.1	504 (12)	33	27 ± 5
Wells in the Regional aquifer in the Rialto-Colton subbasin within the mapped plume								
1N/5W-21N2	PW-2	1.4 ± 0.1	−16.9 ± 0.4	−8.9 ± 0.3	0.0 ± 0.1	118 (4)	22	21 ± 0
1N/5W-21P2	PW-3	1.1 ± 0.2	−18.0 ± 0.2	−9.4 ± 0.2	0.1 ± 0.1	192 (17)	15	15 ± 0
1N/5W-33B1	N-10D	0.5	−14.1 ± 0.5	−7.2 ± 0.2	0.2 ± 0.1	3640 (200)	1.9	1.6 ± 0.2
1N/5W-34B2	Rialto 02	0.2	−20.3 ± 0.2	−10.7 ± 0.2	0.0 ± 0.0	NA	51	51 ± 1
1N/5W-34B2	Rialto 02 (800′)	0.3	−20.1 ± 0.1	−10.6 ± 0.0	0.0 ± 0.0	NA	35	35 ± 1
1N/5W-34G4	PW-5D	0.7 ± 0.4	−17.6 ± 0.6	−9.3 ± 0.3	0.0 ± 0.1	82 (9)	1150	NA
1N/5W-34M1	Rialto 03	0.6 ± 0.3	−15.2 ± 0.1	−8.0 ± 0.3	0.0 ± 0.2	687 (14)	11	12 ± 0
1N/5W-34M1	Rialto 03 (670′)	0.6	−14.4 ± 0.1	−7.6 ± 0.1	0.0 ± 0.0	502 (23)	11	11 ± 0
1S/5W-02B3	PW-9C	1.3	−16.1 ± 0.3	−8.5 ± 0.1	0.0 ± 0.1	127 (18)	341	NA
1S/5W-02G1	Rialto 06	1.3 ± 0.3	−16.9 ± 0.2	−8.8 ± 0.2	0.1 ± 0.1	86 (4)	226	239 ± 13
1S/5W-02G1	Rialto 06 (480′)	1.0	−17.1 ± 0.0	−9.1 ± 0.1	−0.1 ± 0.1	194 (30)	198	206 ± 13
1S/5W-02G1	Rialto 06 (560′)	1.1	−15.7 ± 0.2	−8.3 ± 0.2	0.0 ± 0.1	310 (70)	109	115 ± 13
1S/5W-03A1	Rialto 04	1.1 ± 0.1	−17.6 ± 0.2	−9.2 ± 0.3	0.0 ± 0.2	131 (3)	72	73 ± 2
Wells outside the mapped plume								
1N/5W-17K2	WVWD 24	1.5 ± 0.4	−8.4 ± 0.3	−3.2 ± 0.3	1.2 ± 0.1	6021 (110)	0.3[a]	0.3 ± 0.0j
1N/5W-27D1	Rialto 01	−0.2 ± 0.1	−15.9 ± 0.2	−8.2 ± 0.1	0.2 ± 0.0	2660 ± 127	3.7	3.8 ± 0.5
1N/5W-33N1	F-49A	−2.4 ± 0.0	−8.5 ± 1.0	−1.7 ± 0.4	2.8 ± 0.2	28,900 (1600)	0.4[a]	NA
1S/4W-18G1	Colton 15	−12.3 ± 0.7	−4.6 ± 0.1	6.2 ± 0.1	8.6 ± 0.1	1590 (40)	3.2	3.3 ± 0.1
1S/5W-02K1	WVWD 11	−0.5 ± 0.4	−15.3 ± 0.6	−7.1 ± 0.3	1.0 ± 0.2	66 (3)	9.7	11 ± 1
1S/5W-05A5	F-10C	−4.3 ± 0.2	−9.8 ± 0.5	−1.8 ± 0.2	3.4 ± 0.1	10,200 (400)	0.9[a]	NA
1S/5W-13B5	13B1-5 (RHSW 5)	−9.8	−7.1 ± 0.1	3.1 ± 0.0	6.9 ± 0.0	2210 (160)	4.4	4.2 ± 0.1
1N/5W-32A1	F-13A	−5.5 ± 0.2	−4.8 ± 0.0	2.1 ± 0.2	4.7 ± 0.2	24,200 (1200)	0.4[a]	0.4 ± 0.0j
Wells in the Chino (or Arlington) subbasins								
1S/5W-23A1	WVWD 42	−10.3 ± 0.1	−7.0 ± 0.0	3.5 ± 0.1	7.1 ± 0.1	1785 ± 134	1.4	1.4 ± 0.0
1N/5W-32N1	F-26A	−9.7	−8.3 ± 0.0	1.7 ± 0.0	6.1 ± 0.0	5450 (130)	2.0	1.5 ± 0.2
1N/5W-32N1	F-26A (800′)	−9.9	−8.4 ± 0.1	1.7 ± 0.0	6.2 ± 0.0	5140 (90)	1.6	1.5 ± 0.1
1S/5W-04N1	F-4A	−11.8 ± 0.3	−7.9 ± 0.2	3.4 ± 0.0	7.6 ± 0.1	1380 (30)	5.8	5.9 ± 1.7
1S/5W-04N1	F-4A (J613; 2007 sample)	−11.9	−8.0	3.3	7.6	NA	12	NA
1S/5W-07R1	F-35A	−11.1	−9.4 ± 0.1	1.4 ± 0.0	6.4 ± 0.1	415 (15)	0.6	2.4 ± 0.4
1S/5W-14B1	Chino 02	−11.1	−6.8 ± 0.2	3.7 ± 0.1	7.4 ± 0.0	780 (40)	2.1	1.2 ± 0.8
1S/6W-23D2	F-17B	−13.5 ± 0.0	−6.6 ± 0.3	4.7 ± 0.2	8.2 ± 0.1	91 ± 4	22	19 ± 0.7
1S/6W-23D2	F-17B (580′)	−13.0 ± 0.2	−8.0 ± 0.2	3.9 ± 0.2	8.1 ± 0.1	100 (4)	20	18 ± 1

NA - data not available.

Means and standard deviations are provided for all individual analyses per well. When individual values are provided samples were analyzed once.

$\delta^{18}O$ and $\Delta^{17}O$ were analyzed by O_2-DI-IRMS(+N_2). See Equation 4 for definition of $\Delta^{17}O$.

j - estimated value between the MDL and PQL by IC.

"Column influent" samples were collected intermittently over a period of hours to days while isotope samples were being loaded onto columns.

"Single" samples were collected once when samples for other chemical and isotopic analyses were collected (Izbicki et al., 2015).

For ^{36}Cl, values in parentheses are laboratory reported uncertainty for individual samples while ± values are standard deviations for multiple analyses.

[a] Analysis by IC-MS at Texas Tech University.

columns were removed from the well, sealed in Zip-Loc type bags, placed at 4 °C (or on ice), and shipped to the University of Illinois at Chicago (UIC) for ClO_4^- extraction and purification. In many instances, two or more (up to 8) columns were set up at a single well to collect enough ClO_4^- for stable isotope analysis from low-concentration waters, and to provide replicate samples to evaluate method reproducibility.

As part of this study, laboratory experiments were conducted to evaluate effects of ClO_4^- adsorption to IX resin and column breakthrough on values of $\delta^{37}Cl$, $\delta^{18}O$ and $\Delta^{17}O$, as described in Supporting Data, Section S5.

2.2. Aqueous perchlorate concentrations

Aqueous ClO_4^- concentrations were analyzed by ion-chromatography at the Aptim laboratory in Lawrenceville, NJ using U.S. EPA Method 314.0 (Hautman et al., 1999). Concentrations of ClO_4^- below the detection limit for that method (0.5 µg/L), were analyzed at Texas Tech University in Lubbock, TX, by ion-chromatography mass-spectrometry (ICMS) (US EPA Method 332.0) which has a detection limit of 0.1 µg/L (Hedrick et al., 2005).

2.3. Purification of ClO_4^- for stable isotope analysis

Preparation of ClO_4^- trapped on the IX resin for chlorine and oxygen isotope ratio analysis involved elution and recovery of ClO_4^- from the resin, followed by separation of ClO_4^- from other materials trapped on the IX resin, including a variety of anions and organic compounds. Briefly, the key steps in the extraction and purification method were as follows: (1) the resin was washed ultrasonically with

deionized water (DIW) and flushed with several pore volumes of 4M HCl to remove adsorbed SO_4^{2-}, NO_3^-, HCO_3^-, and humic substances, but not ClO_4^- which is more strongly held by the bifunctional resin than most other anions or organics; (2) ClO_4^- was eluted from the resin bed using 1 M $FeCl_3$-4M HCl solution (Gu et al., 2001, 2011); (3) eluted ClO_4^- was purified by a series of cation exchange, oxidation, and evaporation steps; (4) KOH was added to precipitate $KClO_4$ for isotopic analysis; and (5) $KClO_4$ crystals were washed with methanol and their purity was measured by ion chromatography (IC). Further details on sample purification are provided in Supporting Data, Section S2.

2.4. Analysis of oxygen and chlorine isotope ratios in perchlorate

After the $KClO_4$ was purified according to the procedures described in the previous section, it was analyzed for O and Cl isotopic composition by isotope-ratio mass spectrometry (IRMS) according to procedures described previously (Hatzinger et al., 2011; Sturchio et al., 2014; Böhlke et al., 2017). Details concerning the specific IRMS methods, reference materials, and calibration schemes are given by Böhlke et al. (2017) and in Supporting Data, Section S2.

Stable O and Cl isotope data are reported as follows:

$$\delta^{18}O = R(^{18}O/^{16}O)_{sample}/R(^{18}O/^{16}O)_{VSMOW} - 1 \qquad (1)$$

$$\delta^{17}O = R(^{17}O/^{16}O)_{sample}/R(^{17}O/^{16}O)_{VSMOW} - 1, \qquad (2)$$

$$\delta^{37}Cl = R(^{37}Cl/^{35}Cl)_{sample} / R(^{37}Cl/^{35}Cl)_{SMOC} - 1 \qquad (3)$$

$$\Delta^{17}O = [(1 + \delta^{17}O) / (1 + \delta^{18}O)^{0.525}] - 1. \qquad (4)$$

where $\Delta^{17}O$ is an expression of non-mass-dependent "^{17}O excess" that is calculated from measured $\delta^{18}O$ and $\delta^{17}O$ values. Alternative definitions of "^{17}O excess" ($\Delta^{17}O$, $^{17}\Delta$, etc.) generally would yield values within approximately ± 0.1‰ for samples analyzed in the current study.

Analyses of samples were calibrated by analyzing $KClO_4$ isotopic reference materials USGS37 and USGS38, which were prepared specifically for calibration of ClO_4^- isotopic analyses (Böhlke et al., 2017). For consistency with published data, ClO_4^- calibration values used for data normalization in the current study were consistent with those reported previously (Böhlke et al., 2003): for USGS37, $\delta^{18}O = -17.00‰$, $\delta^{17}O = -8.96‰$, and $\delta^{37}Cl = +0.6‰$; for USGS38, $\delta^{18}O = +52.5‰$ and $\delta^{17}O = +102.5‰$, and $\delta^{37}Cl = -87.2‰$. Normalization was done by assuming no uncertainty in these values (to permit subsequent re-normalization if necessary); analytical uncertainties were estimated by analyzing multiple sample aliquots in different batches, thus incorporating random uncertainties in raw data for both samples and reference materials. Typical reproducibilities (1-σ) for analyses of reference materials were on the order of ± 0.1–0.3‰ for $\delta^{18}O$, $\delta^{17}O$, and $\delta^{37}Cl$, and ± 0.1–0.2‰ for $\Delta^{17}O$. Reproducibilities for purified field samples were similar or slightly larger (Table 1).

2.5. Analysis of ^{36}Cl in ClO_4^-

Analysis of ^{36}Cl in ClO_4^- was performed by accelerator mass spectrometry (AMS) using Cl^- derived from ClO_4^-. The $^{36}Cl/Cl$ mole fractions were determined at the Purdue Rare Isotope Measurement Laboratory (PRIME) at Purdue University (www.physics.purdue.edu/primelab). The procedure used to produce Cl^- for AMS was the same as that described for IRMS in Supporting Data, Section S2.1 to the point of AgCl precipitation, washing, and drying of crystals (i.e., prior to reaction with CH_3I). A portion of the sample prepared to this step for Cl stable isotopic analysis was saved for ^{36}Cl analysis. The AgCl was subsequently re-dissolved and the Cl^- purified twice by anion chromatography (using a method developed by the PRIME Lab at Purdue University; http://www.physics.purdue.edu/primelab/AMSQAQC/chemProc004.pdf) to remove trace amounts of S that might cause isobaric interference at mass 36. Purified Cl^- was then re-precipitated as AgCl for AMS measurement. Analyses of seawater Cl^- provided a

reference datum of $^{36}Cl/Cl$ with a value of 0.5×10^{-15} (Argento et al., 2010).

3. Results and discussion

3.1. ClO_4^- concentrations in groundwater wells

Measured concentrations of ClO_4^- in Study Area groundwater ranged from 0.3 µg/L to 1150 µg/L in wells that were sampled for ClO_4^- isotopes (Table 1). Most of the wells with concentrations above the California Maximum Contaminant Level (MCL) of 6 µg/L were located within the two mapped ClO_4^- plumes, although ClO_4^- was detected at 22 µg/L in Well F-17B in the Chino subbasin (Fig. 1). In general, the average influent concentrations to the IX columns used to collect ClO_4^- for isotopic analysis (which were measured several times while water was passing through the columns) were similar to the individual samples taken separately from each well for ClO_4^- analysis (Table 1). A statistical analysis of the variation of ClO_4^- concentration entering the columns with time (Izbicki et al., 2015) showed influent ClO_4^- concentrations did not change greatly with time in water from wells in the regional aquifer within the Rialto-Colton subbasin or the Chino subbasin, but ClO_4^- concentrations were more variable in water from wells in the perched aquifer underlying the Rialto-Colton subbasin.

3.2. Isotope results for ClO_4^-

The Cl and O stable isotope results for ClO_4^- in Study Area well samples are provided in dual isotope plots in comparison to published data for synthetic, Atacama, and selected indigenous natural ClO_4^- samples in Fig. 2 and Fig. 3. The indigenous source samples are from published data for natural groundwater ClO_4^- samples from the Southern High Plains (SHP) of western Texas and eastern New Mexico, and the Middle Rio Grande Basin (MRGB) of central New Mexico (Sturchio et al., 2006; Jackson et al., 2010). Samples of Death Valley caliche salts are also included in Fig. 2, but these samples were excluded from consideration as a potential indigenous endmember in the Rialto area because of (1) the seemingly limited geographic distribution of these caliche deposits, (2) the fact that ClO_4^- having isotopic composition similar to that of the caliche has not been detected in the regional groundwater (Sturchio et al., 2014), and (3) data regressions in the current study were more consistent with SHP/MRGB-type background ClO_4^- (see below). A more detailed description of indigenous ClO_4^- in these areas is provided in Supporting Data, Section S1. Isotope values ($\delta^{37}Cl$, $\delta^{18}O$ $\Delta^{17}Cl$, and $^{36}Cl/Cl$) from the Study Area samples are plotted with respect to the inverse of the measured ClO_4^- concentrations in Fig. 4 to illustrate potential mixing and dilution trends. In this figure, the isotope source values are from Fig. 2, and indigenous sources (SHP and MRGB) are represented by boxes that encompass their isotopic values and concentrations in groundwater under natural conditions (Fram and Belitz, 2011). Average isotope values and ClO_4^- concentrations in the column influent are provided in Table 1.

In general, ClO_4^- from all three proposed sources was present in varying proportions in Study Area groundwater (Figs. 2–4). Samples having relatively high ClO_4^- concentrations (values of inverse ClO_4^- concentration < 1 L/µg, i.e. ClO_4^- concentration > 1 µg/L) generally plot near a single dominant ClO_4^- source, either synthetic or Atacama (Fig. 4), whereas samples having lower concentrations commonly indicate mixtures with varying fractions of indigenous natural ClO_4^-. These relations are consistent with the presence of low background concentrations of indigenous ClO_4^-, toward which the isotopic compositions of ClO_4^- mixtures converge as fractions of the other two ClO_4^- sources approach zero (Fig. 4).

To facilitate discussion of results, hypothetical mixing relations among three potential ClO_4^- endmembers (synthetic, Atacama, indigenous) are plotted with the Study Area stable isotope data ($\delta^{37}Cl$ vs
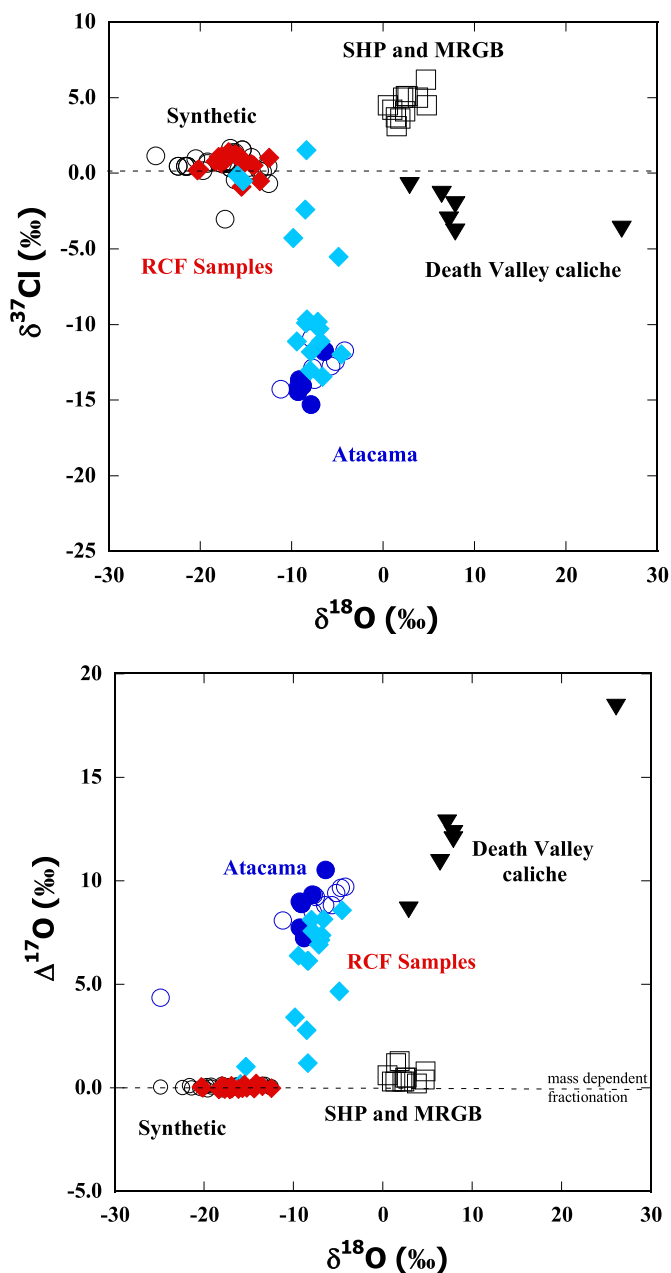
Fig. 2. Comparison of δ^{37}Cl versus δ^{18}O (top panel) and Δ^{17}O versus δ^{18}O (bottom panel) in ClO$_4^-$ from Study Area groundwater samples (diamonds) and other published data. Red closed diamonds indicate wells within the mapped ClO$_4^-$ plume areas and light blue closed diamonds indicate wells outside the mapped plume areas (Table 1; Fig. 1; Izbicki et al., 2015). Other data are for synthetic ClO$_4^-$ (open black circles), natural Atacama ClO$_4^-$ (open blue circles for field samples and closed blue circles for Atacama nitrate fertilizer samples), and indigenous natural ClO$_4^-$ of the southwestern U.S. including Southern High Plains (SHP) and Middle Rio Grande Basin (MRGB) groundwater (black open squares) and Death Valley caliche (black triangles). ClO$_4^-$ isotope data from Bao and Gu (2004); Böhlke et al., 2005; Sturchio et al., 2006, 2012a; Böhlke et al., 2009; Jackson et al., 2010; Hatzinger et al., 2011, 2013. (For interpretation of the references to colour in this figure legend, the reader is referred to the Web version of this article.)

δ^{18}O and Δ^{17}Cl vs δ^{18}O) and with ^{36}Cl data (^{36}Cl/Cl vs δ^{37}Cl) in Fig. 5. A similar three-endmember mixing approach was also recently used to determine the dominant source of ClO$_4^-$ in groundwater of the nearby location of Pomona, CA, using δ^{37}Cl, δ^{18}O, and Δ^{17}O data (Sturchio et al., 2014). Characteristics of three ClO$_4^-$ endmembers for the Study Area groundwaters were estimated as follows: (1) The Atacama and
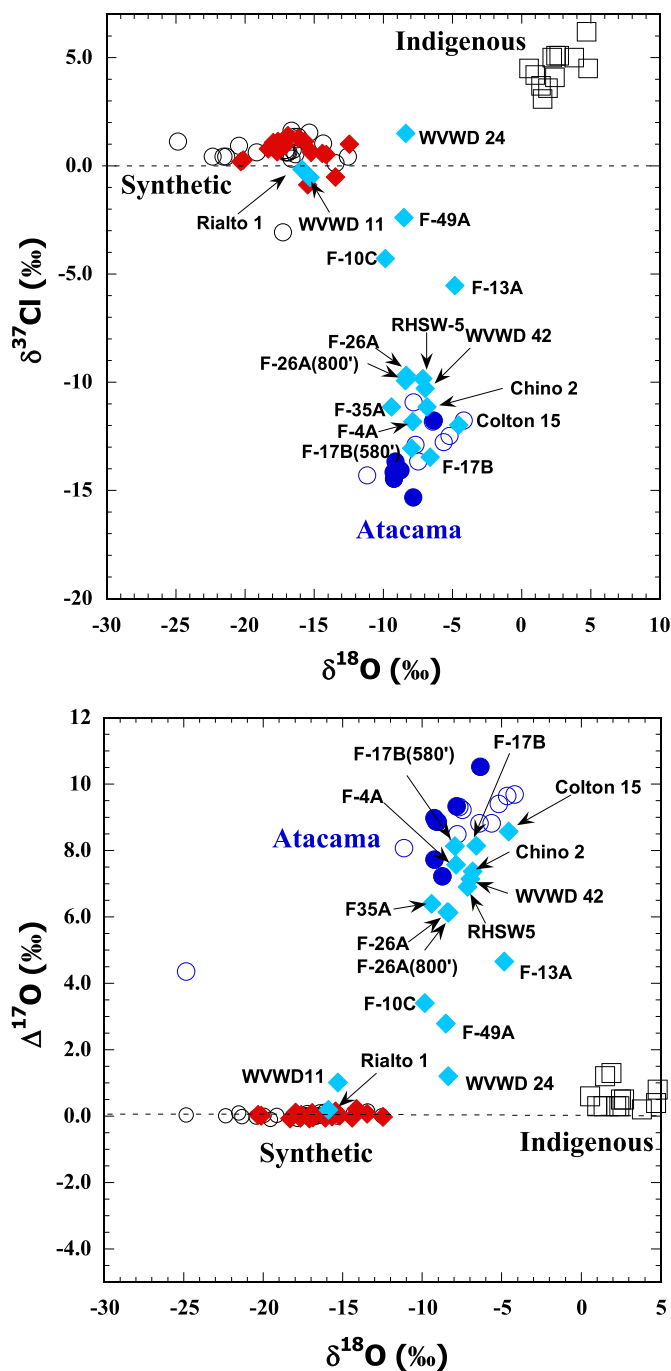

Fig. 3. Comparison of δ^{37}Cl versus δ^{18}O (top panel) and Δ^{17}O versus δ^{18}O (bottom panel) in ClO$_4^-$ from Study Area groundwater samples within the mapped plume areas (red closed diamonds with well designations) and outside the mapped plume areas (light blue closed diamonds) with source data (as described in the caption to Fig. 2). Study Area data are from Table 1. (For interpretation of the references to colour in this figure legend, the reader is referred to the Web version of this article.)

synthetic endmembers were obtained by linear least-squares regressions of δ^{37}Cl, δ^{18}O, and Δ^{17}O values vs. inverse ClO$_4^-$ concentrations. This procedure is based on the assumptions that all samples may have varying amounts of background ClO$_4^-$, no isotope fractionation has occurred, and the Atacama and synthetic endmembers are most likely to dominate at high concentrations (Sturchio et al., 2014). The best-fit regression parameters (slope and intercept, with 2-sigma errors) for all groundwater samples from this study having ClO$_4^-$ concentrations exceeding 1 μg/L were determined using the regression function of

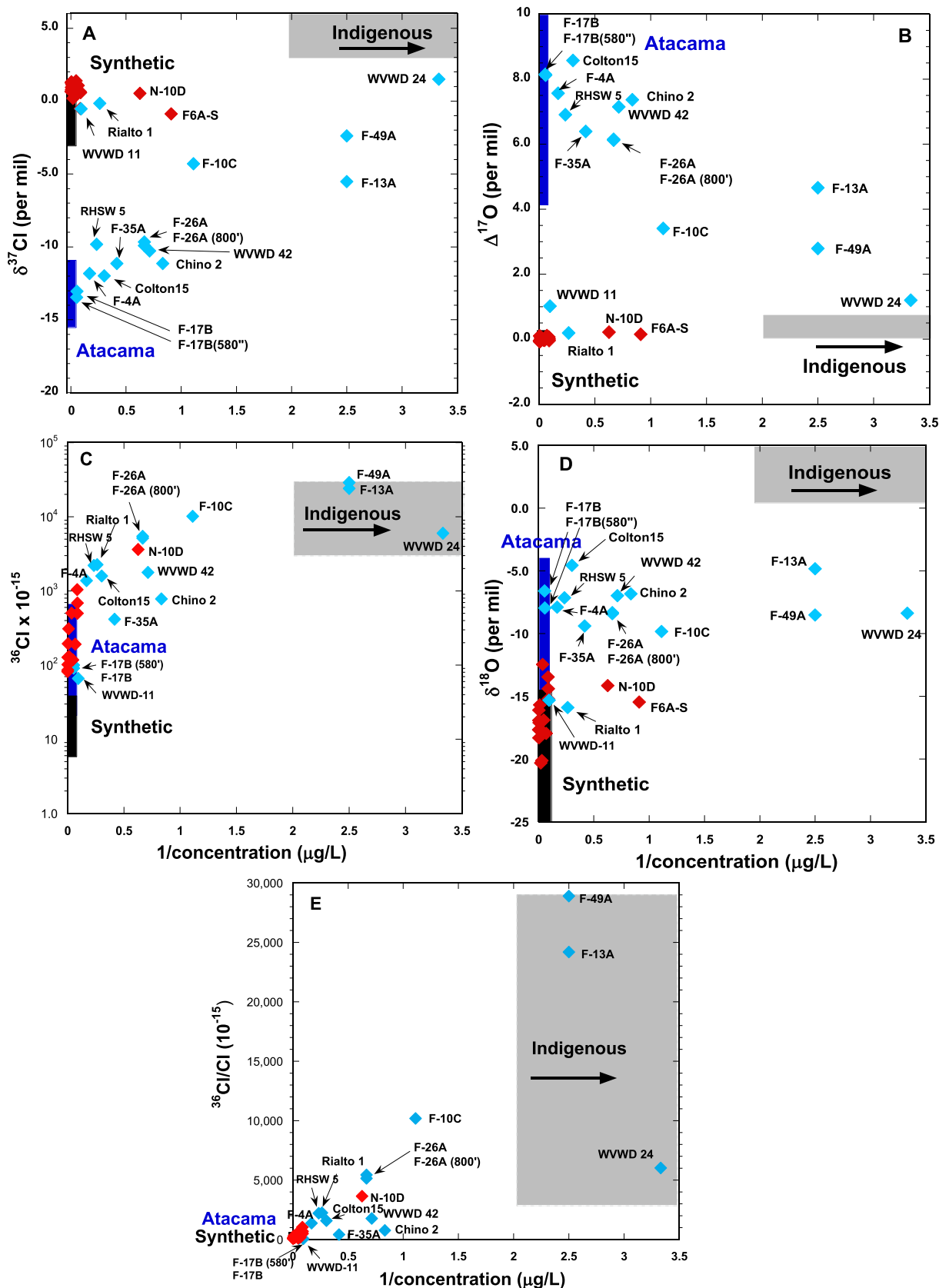**Fig. 4.** Comparison of δ^{37}Cl versus $1/\text{ClO}_4^-$ concentration (panel A), Δ^{17}O versus $1/\text{ClO}_4^-$ concentration (panel B), ^{36}Cl/Cl (x 10^{-15}) on log scale versus $1/\text{ClO}_4^-$ concentration (panel C), δ^{18}O versus $1/\text{ClO}_4^-$ concentration (panel D) and ^{36}Cl/Cl (x 10^{-15}) on linear scale versus $1/\text{ClO}_4^-$ concentration (panel E), with symbols as described in the caption to Fig. 3. The solid bars (including the wide gray bar for indigenous ClO_4^-) represent hypothetical values for the different endmember sources (see Table 2 and text for explanation). The concentration of indigenous ClO_4^- may be lower than indicated on each panel as represented by the arrow. The indigenous ClO_4^- source (gray) includes SHP and MRGB only.
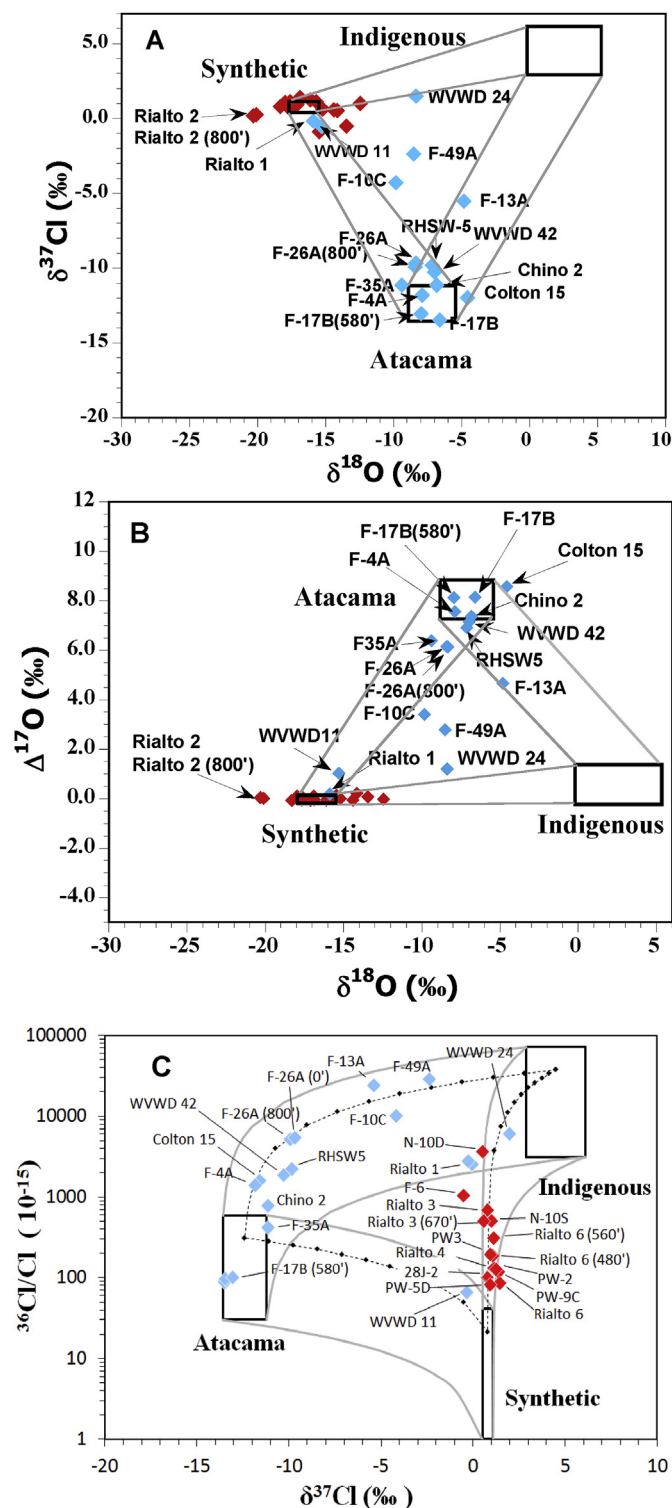
Fig. 5. Comparison of δ^{37}Cl versus δ^{18}O (panel A); Δ^{17}O versus δ^{18}O (panel B) and δ^{37}Cl versus ^{36}Cl/Cl (panel C) in ClO$_4^-$ from Study Area groundwater samples (symbols as in Fig. 3). The sides of each box represent the endmember mean stable isotope ratio value ± 2-sigma error (and, for the ^{36}Cl/Cl ratio, the endmember midpoint value and range) and the gray lines represent mixing zones between the endmember regions. The endmember values were determined as detailed in the accompanying text and are provided in Table 2. The dotted lines in panel C are hypothetical mixing curves with tick marks dividing 10 equal increments along each of the bounding two-component mixing curves.

Table 2

Isotopic compositions of hypothetical endmembers used for analysis of dominant sources in Study Area groundwater. The values in parentheses are 95% confidence limits based on linear regression analysis of data from this study (δ^{37}Cl, δ^{18}O, Δ^{17}O for Atacama and synthetic endmembers) or based on published data from Sturchio et al. (2006) and Jackson et al. (2010) (δ^{37}Cl, δ^{18}O, Δ^{17}O for the indigenous endmember).^{36}Cl/Cl ratios for all three endmembers are the midpoints between highest and lowest reported values from Sturchio et al. (2009), Jackson et al. (2010), and Poghosyan et al. (2014), with ½ of the total range of values for each endmember given in parentheses.

Isotope parameter	Atacama ClO$_4^-$	Synthetic ClO$_4^-$	Indigenous ClO$_4^-$
δ^{37}Cl (‰)	−12.4 (1.2)	0.8 (0.3)	4.5 (1.6)
δ^{18}O (‰)	−7.2 (1.7)	−16.7 (1.1)	2.5 (2.8)
Δ^{17}O (‰)	8.1 (0.8)	0.1 (0.1)	0.6 (0.8)
^{36}Cl/Cl x 10^{-15}	310 (280)	21 (20)	37,200 (34,000)

Values for Atacama and Synthetic endmembers are y-intercepts of best-fit linear regression equations, where x = 1/ClO$_4^-$ (L/μg), as follows:

Atacama δ^{18}O (‰): y = −1.05x −7.17
Atacama Δ^{17}O (‰): y = −2.38x + 8.08
Atacama δ^{37}Cl (‰): y = 3.52x − 12.37
Synthetic δ^{18}O (‰): y = 2.70x − 16.71
Synthetic Δ^{17}O (‰): y = 0.22x + 0.06
Synthetic δ^{37}Cl (‰): y = −1.59x + 0.77

Number of points regressed = 10 for Atacama endmember, 19 for Synthetic endmember.

Microsoft Excel. The concentration cutoff was based on the fact that samples in this concentration range could clearly be seen as having either a dominantly Atacama or dominantly synthetic source, based on all three stable isotope values (see Fig. 4). (2) For the indigenous endmember, as no sample of ClO$_4^-$ obtained from the Study Area was clearly of "pure" indigenous origin, published data for natural groundwater ClO$_4^-$ samples from the SHP and MRGB (Sturchio et al., 2006; Jackson et al., 2010) were used to define its stable isotopic composition (Sturchio et al., 2014). This represents one possible endmember choice, and other alternatives are also discussed below. (3) Because of relatively large variability in measured ^{36}Cl/Cl ratios (particularly for samples relatively enriched in the indigenous endmember), in contrast with the stable isotope ratios, regression analysis did not yield precise estimates of ^{36}Cl/Cl ratios in the dominant endmembers from the Study Area. Therefore, ranges of published values were used to represent ^{36}Cl/Cl ratios of all three endmembers in mixing calculations (Sturchio et al., 2009; Jackson et al., 2010; Poghosyan et al., 2014). The endmember values used for the analysis are provided in Table 2.

The δ^{37}Cl vs. δ^{18}O, Δ^{17}O vs. δ^{18}O, and ^{36}Cl/Cl vs. δ^{37}Cl plots of Study Area sample data, in comparison with the three ClO$_4^-$ source endmembers defined above, indicate that the proposed three-component mixing is capable of accounting for the observed variations in isotopic composition in nearly all samples, given uncertainties and potential variability of endmember characteristics (Fig. 5). Endmember characteristics are shown as boxes with each side being the limit of 2-sigma uncertainty or variability. Mixtures between pairs of endmembers are indicated by gray lines connecting the corners of the endmember boxes. The mixing results in Fig. 5, as well as the Δ^{17}O vs 1/concentration plot in Fig. 4 (panel B), indicate that the Δ^{17}O range of the proposed indigenous Study Area endmember is similar to indigenous ClO$_4^-$ observed in groundwater from the SHP and the MRGB, as well as that in Great Lakes surface water samples (i.e., +0.3 to +2.9‰) rather than the much higher range reported for Death Valley caliche samples (i.e., +8.6 to +18.4‰) (Jackson et al., 2010; Hatzinger et al., 2013; Poghosyan et al., 2014). Additional information about ClO$_4^-$ stable isotope variations in these regions are provided in Supporting Data, Section S1.

To estimate mixing fractions of each of the three ClO$_4^-$ endmembers in Study Area samples, the average values of all stable isotope

ratio analyses for each well (from Table 1) along with endmember values (from Table 2) were used as input for the spreadsheet program *IsoError1_04.xls* as described in Phillips and Gregg (2001) and in the instructions accompanying the spreadsheet. These spreadsheet calculations yielded endmember fractions for each sample, along with their variances, standard errors, and confidence intervals. These calculations are based on assumptions given above, and they account for sample measurement uncertainties and endmember variability and population sizes. Mixing fractions were calculated with 2-sigma error estimates from three pairs of isotope values, $\delta^{37}Cl$ vs. $\delta^{18}O$, $\Delta^{17}O$ vs. $\delta^{18}O$, and $^{36}Cl/Cl$ vs. $\delta^{37}Cl$. The 95% confidence limits (maximum and minimum mixing fractions) from these calculations are provided in Supporting Data, Tables S2–S4. Mixing fractions calculated from $\delta^{37}Cl$ vs. $\delta^{18}O$ generally agree with those calculated from $\Delta^{17}O$ vs. $\delta^{18}O$; there is a cluster of samples near the Atacama endmember, a cluster of samples near the synthetic endmember, and a few intermediate mixed samples that are also the samples having the lowest total ClO_4^- concentrations. Some calculated maximum values of mixing fractions at a 95% confidence interval exceeded 1.0 (with a maximum value of 1.1) and a few of the minimum values were negative at a 95% confidence limit (with a minimum value of -0.2), reflecting uncertainties in the endmember characteristics. The dominant sources indicated by the $^{36}Cl/Cl$ vs $\delta^{37}Cl$ mixing analysis were generally consistent with those determined using the stable isotope pairs. The data also indicated minor fractions of indigenous ClO_4^- in many of the samples as is apparent in Figs. 4 and 5 and discussed in more detail later in this section.

Measured values of $\delta^{18}O$, $\Delta^{17}O$, and $\delta^{37}Cl$ were consistent with those of synthetic ClO_4^- sources for all sampled wells in a perched aquifer within the two mapped ClO_4^- plume areas (28J-2, F-6, F6A-S, N-10S) (see Izbicki et al. (2015) for further details of aquifer characteristics). Similarly, isotopic data from wells in the underlying regional aquifer within the mapped plume areas also were consistent with a dominantly synthetic source (with minimum mixing fractions generally ranging from 60 to 90% and maximum fractions at 100–110% using a 95% confidence interval), including PW-2, PW-3, Rialto 2, Rialto 2 (880′), PW-5D, Rialto 3, Rialto 3 (670′), PW-9C, Rialto 6, Rialto 6 (480′), Rialto 6 (560'), and Rialto 4. All of these samples had mean $\delta^{37}Cl$ values between -1.0 and $+1.5‰$ and $\Delta^{17}O$ values between -0.1 and $+0.2‰$, consistent with dominantly synthetic ClO_4^-. The $\delta^{18}O$ values varied from -12.5 to $-20.3‰$, also within the range previously reported for synthetic ClO_4^-. However, the relatively wide range in $\delta^{18}O$ values for these samples also appears to reflect mixing with indigenous ClO_4^- (see next paragraph) in addition to possible variation in synthetic source isotopic ratios.

Some data from wells within the mapped contaminant plume indicate minor fractions (0%–~10%) of indigenous natural ClO_4^-, based upon the values of $^{36}Cl/Cl$ in the samples compared to synthetic ClO_4^- sources (Fig. 5, Table S4). Minor indigenous fractions were difficult to resolve in the stable isotope endmember mixing model results, because these fractions were small compared to the uncertainties associated with the stable isotope mixing calculations (Tables S2 and S3), whereas the indigenous source is more readily identified by its much higher ^{36}Cl abundance. Hypothetical mixing curves for $^{36}Cl/Cl$ and $\delta^{37}Cl$ with endpoints in synthetic, Atacama, and indigenous natural ClO_4^- in Fig. 5 (panel C) highlight an apparent trend of increasing indigenous ClO_4^- in the data array from PW5D (0%) to N10-D ($\sim 10\%$). $\delta^{18}O$ values slightly higher than the proposed synthetic endmember (with a $\delta^{18}O$ value of $-16.7 \pm 1.1‰$) are also consistent with varying fractions of indigenous natural ClO_4^- in some of the same samples (Fig. 5).

Within the mapped plume areas, samples having larger apparent fractions of indigenous ClO_4^- based on elevated $\delta^{18}O$ and $^{36}Cl/Cl$ ratios tended also to have lower total ClO_4^- concentrations (Fig. 6), consistent with varying fractions of a low-concentration background source. According to a regional statistical study (Fram and Belitz, 2011), in the absence of anthropogenic sources or localized flushing of ClO_4^- from the vadose zone by irrigation or other artificial recharge
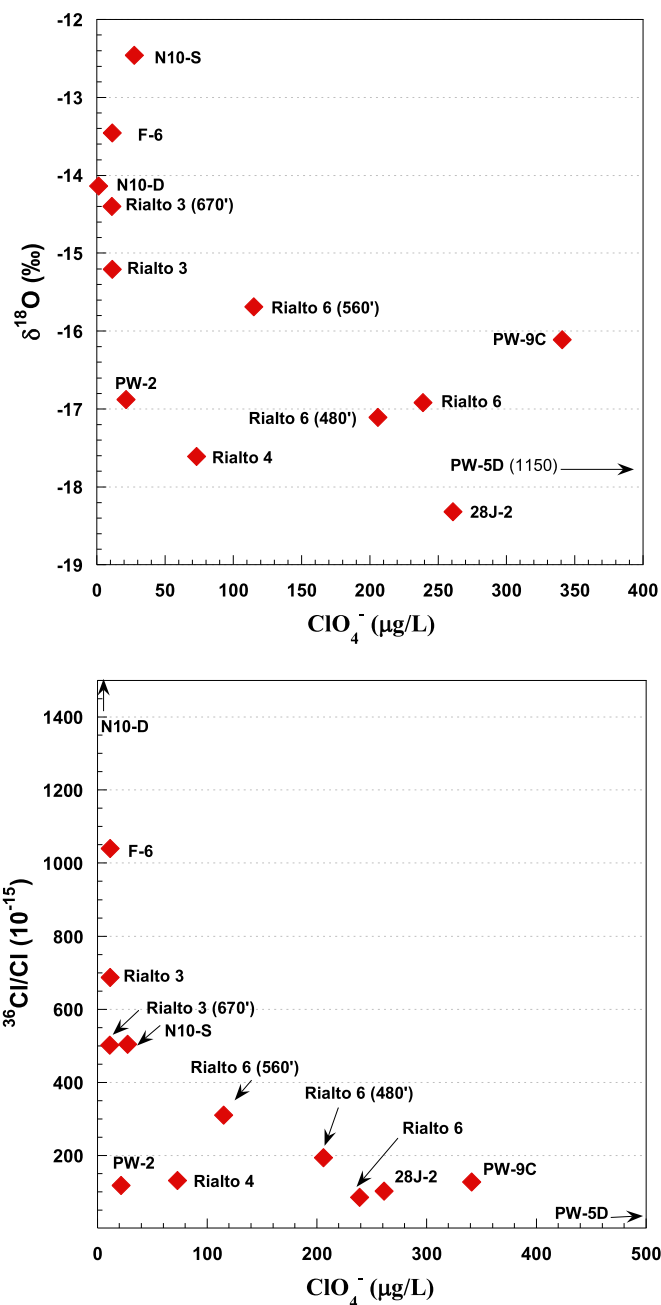

Fig. 6. Comparison of $\delta^{18}O$ value (‰) versus ClO_4^- concentration (top panel) and $^{36}Cl/Cl$ ratio vs ClO_4^- concentration (bottom panel) for all wells located within the mapped ClO_4^- plume areas for which both values are available.

processes, concentrations of indigenous natural ClO_4^- in groundwater in arid/semiarid areas of the southwestern U.S. are likely to be less than 1 μg/L. Where accumulated salts are flushed from the vadose zone, natural ClO_4^- concentrations can be much higher, sometimes exceeding 4 μg/L and occasionally reaching > 50 μg/L, as reported for irrigated agricultural regions of the SHP (Jackson et al., 2005; Rajagopalan et al., 2006; Rao et al., 2007). Some of the variability observed in Figs. 5 and 6 may reflect differing concentrations of natural background ClO_4^- in these wells and variability in synthetic and indigenous endmember isotope values; nevertheless, the general relations are consistent with relatively low background concentrations (< 0.5 μg/L). The sample from N-10D, with a total ClO_4^- concentration of 1.6 μg/L, had a larger apparent fraction of indigenous natural ClO_4^- ($\sim 10\%$, based on its $^{36}Cl/Cl$ ratio) than most other wells within the

area of the mapped contaminant plumes, possibly indicating this sample included groundwater from beneath the contaminant plumes, which would be consistent with the relatively deep screened interval from which the sample was collected (see Izbicki et al., 2015).

Downgradient from the two mapped plumes in the southeastern direction, parallel to the Rialto-Colton Fault, the dominant source of ClO_4^- appears to shift from synthetic to Atacama, presumably because of past fertilizer use in the recharge areas for these groundwaters. The ClO_4^- in WVWD 11 appeared to be predominantly synthetic ($\geq 60\%$ based on mixing fraction analysis), but with a significant fraction of Atacama ClO_4^- based upon its $\Delta^{17}O$ value of $\sim +1‰$, compared to $< +0.2‰$ for all other samples collected in the mapped plume area. WVWD 11 also had a lower $\delta^{37}Cl$ value ($-0.5‰$) than most of the wells that appeared to have predominantly synthetic ClO_4^- (average $+0.6 \pm 0.6‰$), consistent with a minor Atacama component. Farther downgradient, wells 13B1-5 (RHSW-5) and Colton 15 had ClO_4^- that was predominantly Atacama ($\geq 70\%$), based upon their low $\delta^{37}Cl$ values (-9.8 and $-12.0‰$, respectively) and elevated $\Delta^{17}O$ values ($+6.9$ and $+9.0‰$, respectively). The combination of low $\delta^{37}Cl$ values and high $\Delta^{17}O$ values in these samples is characteristic of Atacama-derived ClO_4^- (Böhlke et al., 2005, 2009; Jackson et al., 2010; Sturchio et al., 2012a, 2012b, 2014). The non-Atacama ClO_4^- in these samples (RHSW-5, Colton 15) appears to be largely indigenous, based upon elevated $^{36}Cl/Cl$ values and other correlations.

Samples from the Chino subbasin, southwest of the Rialto-Colton Fault, including those from wells WVWD 42, F-17B, F-35A, F-4A, Chino 2, and F-26A, also had isotopic characteristics indicating predominantly Atacama ClO_4^- ($\geq 70\%$ based on mixing fraction calculations), including elevated values of $\Delta^{17}O$ ($+6.1$ to $+8.2‰$) and low values of $\delta^{37}Cl$ (-6.6 to $-9.4‰$). The finding of ClO_4^- derived from Atacama fertilizer in the Chino subbasin is consistent with data from previous studies examining ClO_4^- sources in the western region of this subbasin using the triple stable isotope approach (Sturchio et al., 2008, 2012b, 2014). Similarly, Atacama ClO_4^- was identified recently in a number of wells in Riverside, CA in the vicinity of the San Bernardino Airport to the southeast of the Study Area along the Santa Ana River using the stable isotope approach (Sturchio et al., 2012a, 2012b). In that area, Atacama ClO_4^- was identified in wells outside a plume of synthetic ClO_4^-. Minor fractions of indigenous natural ClO_4^- also were indicated in some of the Riverside wells based on the stable isotope values.

The detection of Atacama ClO_4^- in the Study Area on both sides of the Rialto-Colton Fault and across the Chino subbasin is consistent with the past agricultural history of this area, and with anecdotal evidence of the application of Atacama nitrate fertilizer throughout this region (Sturchio et al., 2008, 2012a, 2012b, 2014). A 1949 land use map (GeoLogic Associates, 2002) showing agricultural regions in the Chino Basin, and covering a substantial portion of the Study Area, is provided in Fig. S5. This map shows the locations of irrigated vineyards, and irrigated and non-irrigated citrus orchards. Based on the history of this region, it is likely that these areas were in agriculture for at least a few decades before this 1949 map, when application of Atacama fertilizer was common. Additional historical citrus production along Lytle Creek that is not shown on this figure has also been documented (GeoLogic Associates, 2002). Peak citrus production in the Chino Basin occurred during the period 1930–1950 (USDA, 2013).

Well WVWD 24 (northernmost well in Fig. 1) was initially selected for sampling as a possible representative of uncontaminated ("background") conditions, based upon its location far upgradient of the two ClO_4^- plume source areas, its low ClO_4^- concentration ($\sim 0.3 \mu g/L$), and its potential for recharge from the San Gabriel Mountains (Izbicki et al., 2015). It was hypothesized that wells in this part of the Study Area were most likely to contain local indigenous natural ClO_4^-, rather than synthetic or Atacama ClO_4^-. Three additional wells (monitoring wells F-27A, F-33A, and F-42A) to the north of WVWD 24 were considered for background sampling, but ClO_4^- concentrations in these wells (0.10, 0.11, and 0.14 $\mu g/L$, respectively) were considered to be

too low to obtain adequate ClO_4^- for isotopic analysis.

Based on our endmember selections for mixing analysis, isotope data for ClO_4^- from WVWD 24 indicated that this well contained a mixture composed primarily of indigenous natural ClO_4^- and synthetic ClO_4^-. The sample had a $\delta^{18}O$ value of $-6.8‰$, which is between the estimated endmember values of synthetic ClO_4^- ($-16.7‰$) and indigenous natural ClO_4^- ($+2.5‰$) listed in Table 2. The WVWD 24 sample had a $\Delta^{17}O$ value of $+1.2‰$, which is within the range reported for indigenous natural ClO_4^- in the southwest US (Jackson et al., 2010) and slightly lower than that for samples from the Great Lakes (Poghosyan et al., 2014). Finally, the $^{36}Cl/Cl$ ratio of WVWD 24 (6021×10^{-15}) placed it within the lower end of the range reported for indigenous natural ClO_4^- (Sturchio et al., 2009; Poghosyan et al., 2014). All of these observations, plus the higher ClO_4^- concentration in WVWD-24 of 0.3 $\mu g/L$ compared to concentrations ranging from 0.1 to 0.14 $\mu g/L$ in other nearby wells, are consistent with a synthetic-indigenous mixture in WVWD 24.

Tritium (^3H) was detected in WVWD 24 at 10.6 pCi/L (Izbicki et al., 2015), indicating that it contained at least some modern (post-bomb) recharge water. WVWD-24 is upgradient from the identified source areas of the two mapped ClO_4^- plumes (Fig. 1), and it is unlikely to have acquired synthetic ClO_4^- from those source areas by groundwater flow (Izbicki et al., 2015). If synthetic ClO_4^- was present in WVWD 24, as indicated by the isotope data, it may have originated from other commercial sources, such as road flares, fireworks, or blasting explosives, each of which could have contributed to groundwater contamination in this area, as they apparently have elsewhere in the U.S. (e.g., Böhlke et al., 2009; Munster and Hanson, 2009; Munster, 2008; Munster et al., 2008; Aziz and Hatzinger, 2008).

An alternative hypothesis is that the sample from WVWD 24 represents a local indigenous natural component that is different from the one proposed in the mixing analysis. Additional regional sampling would be required to further evaluate this hypothesis. Moreover, whether ClO_4^- from WVWD 24 was entirely or only partly natural (i.e., indigenous mixed with synthetic), it could represent a regional background ClO_4^- that is present in varying proportions in other wells in the Study Area that are not within the mapped plumes. Mixing calculations based on this assumption could alter the estimated component mixing fractions for some wells, but would not change the interpretation of major ClO_4^- sources in most wells, except a few with very low ClO_4^- concentrations ($< 1 \mu g/L$) where the indigenous fraction is a large component as discussed below.

Three wells not discussed above, F-13A, F-49A, and F-10C, had low ClO_4^- concentrations ranging from 0.4 to 0.9 $\mu g/L$ and appeared to represent mixed ClO_4^- sources. In map view (Fig. 1), well F-13A is near Barrier H (a mapped fault or hydrologic discontinuity), to the south of the RFF site, well F-49A is east of Barrier H, and well F-10C is east of the Rialto-Colton Fault and west of Barrier H. Wells F-10C and F-49A were observed to have perched groundwater cascading downward and mixing with deeper water in the well casing (Izbicki et al., 2015). The perched groundwater may have carried ClO_4^- that was not present in deeper groundwater in these wells. Evaluating all three stable isotopic parameters ($\delta^{18}O$, $\delta^{37}Cl$, $\Delta^{17}O$), and assuming the characteristics of Atacama, synthetic, and indigenous end members as described above, the ClO_4^- in well F-13A appears to consist largely of Atacama and indigenous ClO_4^-, whereas wells F10-C and F49-A appear to have ClO_4^- from all three endmember sources, with no individual component dominating the mixture. Alternatively, if isotope data from WVWD 24 represented a widespread mixed (indigenous $\pm$ synthetic) background ClO_4^- type, then data from F10-C and F49-A could be consistent with mixtures of Atacama and that mixed background type.

Relations between $^{36}Cl/Cl$ and $\delta^{37}Cl$ values (Fig. 5, panel C) generally support the observations above for these wells, but appear to indicate somewhat larger fractions of indigenous ClO_4^- and smaller fractions of synthetic ClO_4^-. These apparent differences could be due to variability associated with the $^{36}Cl/Cl$ ratio of natural ClO_4^-.

Alternatively, it could indicate contributions of anomalously [36]Cl-en-riched indigenous ClO_4^- from the brief period of thermonuclear bomb tests in the western Pacific (1952–1964). Poghosyan et al. (2014) propose that ClO_4^- having [36]Cl/Cl ratios around $1,000,000 \times 10^{-15}$ was widely deposited during that time, based on their measurements of [36]Cl in ClO_4^- from Lake Superior. Most of the samples analyzed in the current study, with the exception of bulk discharge from well F-17B, had measurable [3]H (Izbicki et al., 2015), indicating at least a portion of the water precipitated after 1952. Any bomb-pulse ClO_4^- contribution (if present) would likely be most evident in the lowest-concentration samples (i.e., F-10C, F-13A, F-49A, and WVWD 24); these are the samples having the highest [36]Cl/Cl ratios in the present study. A potential bomb-pulse contribution is partially accounted for in the indigenous endmember used for mixing calculations (Table 2) by inclusion of data from the Great Lakes (Poghosyan et al., 2014). However, it is possible that the [36]Cl/Cl ratio was actually higher than that assumed for our mixing calculations or that the bomb-pulse contribution varied substantially on a well-by-well basis in relation to varying local recharge conditions.

The origin of the apparent synthetic ClO_4^- fraction in wells F-10C and F-49A (based on stable isotope data) is uncertain, as it contributed a maximum of only about 0.6 and 0.2 μg/L, respectively, to the mixtures in the wells based on stable isotope mixing fraction estimates (Tables S2 and S3). Sources of such low concentrations could include upgradient background groundwater (as in WVWD 24), plume-related or non-plume-related ClO_4^- in perched groundwater, or other local contamination. Alternatively, if the ClO_4^- in WVWD 24 was isotopically representative of indigenous natural ClO_4^- in the Study Area, then the apparent synthetic fractions in wells F-10C and F-49A would be reduced or eliminated, as these wells fall reasonably in a mixing line between WVWD 24 and the Atacama endmember based on stable isotope values (Fig. 5). In this case, however, the [36]Cl/Cl ratios in these two samples would be expected to fall between that of WVWD 24 and the Atacama endpoint, rather than being much higher (as in F-49A).

3.3. Depth-dependent ClO_4^- isotope results

Depth-dependent groundwater sampling and isotopic analysis were conducted on five of the production wells in the Study Area: F-17B, F-26A, Rialto 2, Rialto 3, and Rialto 6. This work was conducted as part of the coupled well-bore flow and depth dependent water quality data analysis described by Izbicki et al. (2015). The primary objective of analyzing ClO_4^- isotopes at various depths in these wells was to determine whether different sources were entering the wells at different depth intervals in the aquifer(s) (e.g., synthetic ClO_4^- at the top of the well screen and indigenous ClO_4^- at a deeper screened interval).

Overall, the results showed that the source(s) of ClO_4^- collected from the surface discharge of each of the wells was similar to that collected from a deep interval within the well, or in the case of Rialto 6, from two different depth intervals (Table 1; Fig. 7). Although there were small differences in $\delta^{18}O$ between F-17B (580′) and F-17B (bulk discharge) and between Rialto 6 (480′) and Rialto 6 (560′), these differences did not indicate substantial differences in ClO_4^- source fractions. In general, the major-ion compositions of depth-dependent samples were similar to those of the total surface discharge from each well, with the exception of dissolved oxygen (DO), which generally decreased with depth (Izbicki et al., 2015). Biological degradation of ClO_4^- and associated fractionation of Cl and O isotopes in ClO_4^- are possible under anoxic conditions, particularly if organic carbon or other electron donors are available for growth of ClO_4^--reducing bacteria (e.g., Sturchio et al., 2007; Hatzinger et al., 2013). However, depth-dependent discharge data indicate deeper groundwater with low DO may not contribute substantially to the total discharge from the wells (Izbicki et al., 2015). No evidence of ClO_4^- isotopic fractionation was apparent in the depth-dependent samples. Similarly, no evidence of NO_3^- isotopic fractionation that might be associated with NO_3^-
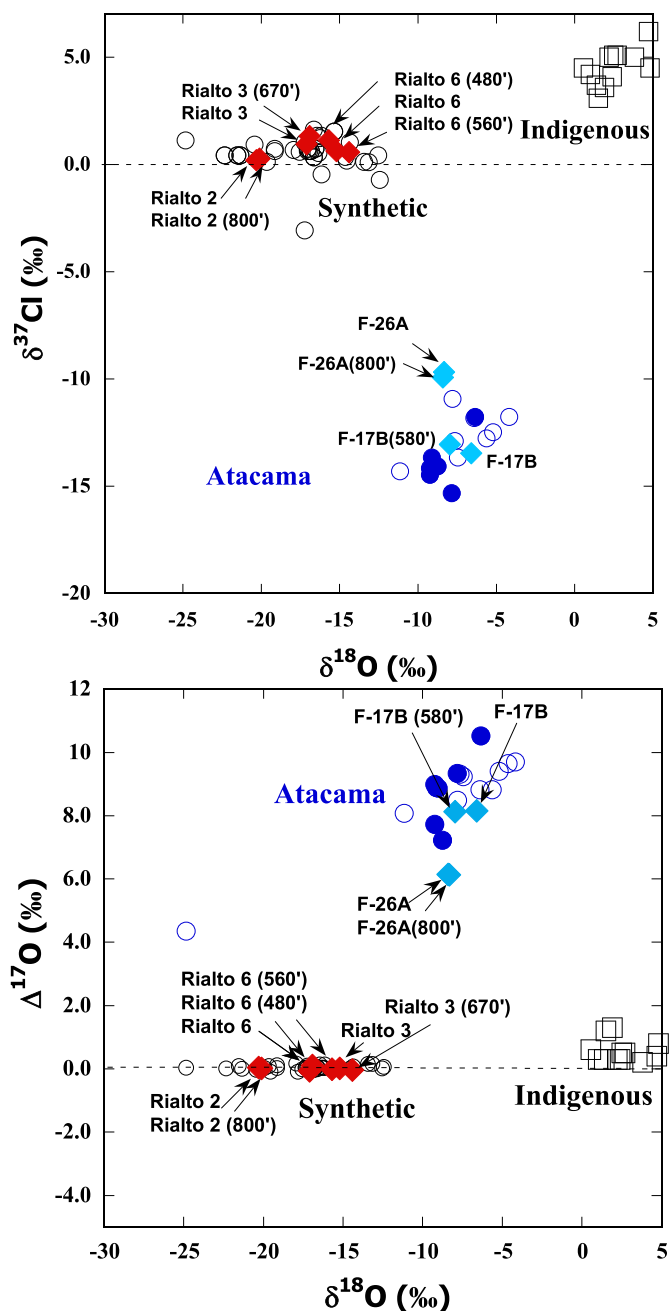

Fig. 7. Comparison of $\delta^{37}Cl$ versus $\delta^{18}O$ (top panel) and $\Delta^{17}O$ versus $\delta^{18}O$ (bottom panel) in ClO_4^- from Study Area groundwater depth-dependent samples (symbols as in Fig. 3) with published data for indigenous natural ClO_4^- of the SHP and MRGB (black open squares), natural Atacama ClO_4^-, (open blue circles for field samples and closed blue circles for Atacama nitrate fertilizer samples) and synthetic ClO_4^- (open black circles). Sources of data for Atacama, Synthetic and Indigenous ClO_4^- as described in Fig. 2. (For interpretation of the references to colour in this figure legend, the reader is referred to the Web version of this article.)

reduction was apparent in the same set of samples (Izbicki et al., 2015). For wells F-26A, F-17B, and Rialto 6, both the deep sampled interval and the bulk discharge had high DO concentrations (> 8 mg/L; Izbicki et al., 2015), indicating the bulk of the sampled groundwater was from the upper oxic part of the aquifer. The DO concentration was low for Rialto 3 at 670' (0.2 mg/L) but there was little or no evidence for biological isotopic fractionation of ClO_4^- or NO_3^- in this sample. Dissolved oxygen data were not available for Rialto 2 with depth.

3.4. Summary and conclusions

This paper describes a comprehensive applied isotopic study of multiple ClO_4^- sources in groundwater. Samples were collected from wells throughout the Rialto-Colton and Chino groundwater subbasins having complex hydrogeology and land use history with multiple sources of ClO_4^- contamination. The dominant source(s) of ClO_4^- in each of these samples was evaluated based on Cl and O stable isotope ratios ($\delta^{37}Cl$, $\delta^{18}O$, $\Delta^{17}O$) and ^{36}Cl abundances in the ClO_4^-. The data indicate that synthetic, Atacama, and indigenous natural ClO_4^- all were present in groundwater of the study area. In general, isotopic data for samples having ClO_4^- concentrations greater than 1 µg/L were consistent with either synthetic or Atacama ClO_4^- sources, whereas isotopic data for samples having concentrations less than 1 µg/L were more likely to indicate mixtures that include substantial indigenous natural ClO_4^- fractions.

Depth-dependent sampling was conducted in several production wells to determine if different sources of ClO_4^- were present in these wells at different depth intervals (e.g., synthetic ClO_4^- in shallow groundwater and indigenous natural ClO_4^- in deep groundwater). The isotopic data generally were similar between the surface discharge of the well and samples collected at depth within the well under pumped conditions, indicating little or no variation in major ClO_4^- source(s) with depth in these wells.

In comparison to previous studies, this one featured comprehensive isotopic characterization of a relatively large number of samples, with multiple tests of sampling and analysis procedures, thus adding support for the isotopic approach to ClO_4^- source identification and apportionment. Data and comparative dual-isotope mixing calculations illustrate the value of measuring all four of the isotopic ratios in each sample ($\delta^{37}Cl$, $\delta^{18}O$, $\Delta^{17}O$, and $^{36}Cl/Cl$) to minimize uncertainty in ClO_4^- sources. Although three stable isotope parameters commonly were sufficient to resolve major sources in many samples, $^{36}Cl/Cl$ values contributed substantially to detection of indigenous natural ClO_4^- components. Additional insights may be gained from further studies, including integrated quadruple-isotope evaluation of endmembers and mixtures, improvements in analytical procedures for low-concentration samples, and an increased database of indigenous natural ClO_4^- occurrences.

Acknowledgments

Appendix A. Supplementary data

Supplementary data related to this article can be found at https://doi.org/10.1016/j.apgeochem.2018.08.020.

References

Argento, D.C., Stone, J.O., Fifield, L.K., Tims, S.G., 2010. Chlorine-36 in seawater. Nucl. Instrum. Meth. Phys. Res. B. 268, 1226–1228.
Aziz, C.E., Hatzinger, P.B., 2008. Perchlorate sources, source identification, and analytical methods. In: Stroo, H.F., Ward, C.H. (Eds.), In Situ Bioremediation of Perchlorate. Springer, New York, pp. 55–77.
Bao, H., Gu, B., 2004. Natural perchlorate has a unique isotopic signature. Environ. Sci. Technol. 38, 5073–5077.
Böhlke, J.K., Hatzinger, P.B., Sturchio, N.C., Gu, B., Abbene, I., Mroczkowski, S.J., 2009. Atacama perchlorate as an agricultural contaminant in groundwater: isotopic and chronologic evidence from Long Island, New York. Environ. Sci. Technol. 43, 5619–5625.
Böhlke, J.K., Sturchio, N.C., Gu, B., Horita, J., Brown, G.M., Jackson, W.A., Batista, J.R., Hatzinger, P.B., 2005. Perchlorate isotope forensics. Anal. Chem. 77, 7838–7842.
Böhlke, J.K., Mroczkowski, S.J., Coplen, T.B., 2003. Oxygen isotopes in nitrate: new reference materials for $^{18}O{:}^{17}O{:}^{16}O$ measurements and observations on nitrate-water equilibration. Rapid Commun. Mass Spectrom. 17, 1835–1846.
Böhlke, J.K., Mroczkowski, S.J., Sturchio, N.C., Heraty, L.J., Richman, K., Sullivan, D., Griffith, K., Hatzinger, P.B., 2017. Stable isotope analysis of oxygen ($^{18}O{:}^{17}O{:}^{16}O$) and chlorine ($^{37}Cl{:}^{35}Cl$) in perchlorate: reference materials, calibrations, methods, and interferences. Rapid Commun. Mass Spectrom. 30, 1–26.
California Department of Food and Agriculture, 1999. Fertilizing Materials Tonnage Report. July-December 1999, Sacramento, CA.
Cunniff, S.E., Cramer, R.J., Maupin, H.E., 2006. Perchlorate: challenges and lessons. In: Gu, B., Coates, J.D. (Eds.), Perchlorate Environmental Occurrences, Interactions, and Treatment. Springer, New York, pp. 1–14.
Dasgupta, P.K., Dyke, J.V., Kirk, A.B., Jackson, W.A., 2006. Perchlorate in the United States. Analysis of relative source contributions to the food chain. Environ. Sci. Technol. 40, 6608–6614.
Dasgupta, P.K., Martinelango, P.K., Jackson, W.A., Anderson, T.A., Tian, K., Tock, R.W., Rajagopalan, S., 2005. The origin of naturally occurring perchlorate: the role of atmospheric processes. Environ. Sci. Technol. 39, 1569–1575.
Dutcher, L., Garrett, A., 1963. Geologic and Hydrologic Features of the San Bernardino Area, California—with Special Reference to Underflow Across the San Jacinto Fault. pp. 114. USGS Water Supply Paper 1419. http://pubs.er.usgs.gov/publication/wsp1419.
Eldridge, J.E., Tsui, D.T., Mattie, D.R., Crown, J., Scott, R., 2000. Perchlorate in Fertilizers. U.S. Air Force Research Laboratories. Wright Patterson AFB, OH.
Ericksen, G.E., 1981. Geology and Origin of the Atacama Nitrate Deposits. U.S. Geological Survey, Washington, D.C Prof. Paper 1188.
Ericksen, G.E., 1983. The Atacama nitrate deposits. Am. Sci. 71, 366–374.
Fram, M.S., Belitz, K., 2011. Probability of detecting perchlorate under natural conditions in deep groundwater in California and the southwestern United States. Environ. Sci. Technol. 45, 1271–1277.
GeoLogic Associates (in association with Bryan A. Stirrat & Associates), 2002. Environmental Audit, Potential Sources of Perchlorate Impacts. Rialto-Colton Groundwater Basin, San Bernardino, California (Anaheim, Calif., variously paged).
GeoLogic Associates, 2003. Perchlorate Investigation in the Vicinity of the Mid Valley Sanitary Landfill, San Bernardino, California. Report Prepared for the County of San Bernardino Waste System Division. (Anaheim, Calif., variously paged).
GeoLogic Associates, 2013. First Quarter (Winter) 2013 Monitoring Report Rialto GWTS Perchlorate and VOC Investigation, San Bernardino County, California. (Anaheim, Calif., variously paged).
Gu, B., Brown, G.M., Maya, L., Lance, M.J., Moyer, B.A., 2001. Regeneration of perchlorate (ClO_4^-)-loaded anion exchange resins by novel tetrachloroferrate ($FeCl_4^-$) displacement technique. Environ. Sci. Technol. 35, 3363–3368.
Gu, B., Brown, G.M., Chiang, C.C., 2007. Treatment of perchlorate-contaminated groundwater using highly selective, regenerable ion-exchange technologies. Environ. Sci. Technol. 41, 6277–6282.
Gu, B., Böhlke, J.K., Sturchio, N.C., Hatzinger, P.B., Jackson, W.A., Beloso Jr., A.D., Heraty, L.J., Bian, Y., Jiang, X., Brown, G.M., 2011. Removal, Recovery and Fingerprinting of Perchlorate by Ion Exchange Processes in Ion Exchange And Solvent Extraction: a Series of Advances, twentieth ed. Taylor and Francis Group, New York, pp. 117–144.
Hatzinger, P.B., Böhlke, J.K., Sturchio, N.C., Gu, B., 2011. Guidance Document: Validation of Chlorine and Oxygen Isotope Ratios to Differentiate Perchlorate Sources and Document Perchlorate Biodegradation. Environmental Security Technology Certification Program, pp. 107. Online. http://www.clu.in.org/download/contaminantfocus/perchlorate/Perchlorate-ER-200509-GD.pdf.
Hatzinger, P.B., Böhlke, J.K., Sturchio, N.C., Gu, B., 2013. Validation of Chlorine and Oxygen Isotope Ratios to Differentiate Perchlorate Sources and Document Perchlorate Biodegradation. Final Report. Environmental Security Technology Certification Program, pp. 176. Online. http://www.serdp.org/Program-Areas/Environmental-Restoration/Contaminated-Groundwater/Emerging-Issues/ER-200509.
Hautman, D.P., Munch, D.J., Eaton, A.D., Haghani, A.W., 1999. Method 314.0 Determination of Perchlorate in Drinking Water Using Ion Chromatography, Revision 1.0. U.S. Environmental Protection Agency, Cincinnati, OH, pp. 49 EPA 815-B-99-003.
Hedrick, E.J., Slingsby, R.l, Munch, D.J., 2005. Method 332.0: Determination of Perchlorate in Drinking Water by Ion Chromatography with Suppressed Conductivity and Electrospray Ionization Mass Spectrometry. U.S. Environmental Protection Agency, Washington, DC Online. https://cfpub.epa.gov/si/si_public_record_report.cfm?dirEntryId=131665.

Izbicki, J., Teague, N.F., Hatzinger, P.B., Böhlke, J.K., Sturchio, N.C., 2015. Groundwater movement, recharge, and perchlorate occurrence in a faulted alluvial aquifer in California (USA). Hydrogeol. J. 23, 467–491.

Jackson, W.A., Böhlke, J.K., Gu, B., Hatzinger, P.B., Sturchio, N.C., 2010. Isotopic composition and origin of indigenous natural perchlorate and co-occurring nitrate in the southwestern United States. Environ. Sci. Technol. 44, 4869–4876.

Jackson, W.A., Anderson, T.A., Harvey, G., Orris, G., Rajagopalan, S., Namgoo, K., 2006. Occurrence and formation of non-anthropogenic perchlorate. In: Gu, B., Coates, J.D. (Eds.), Perchlorate Environmental Occurrences, Interactions, and Treatment. Springer, New York, pp. 49–66.

Jackson, W.A., Anandam, S.K., Anderson, T., Lehman, T., Rainwater, K., Rajagopalan, S., Ridley, M., Tock, R., 2005. Perchlorate occurrence in the Texas southern high plains aquifer system. Ground Water Monit. Remed. 25, 137–149.

Jackson, W.A., Anderson, T.A., Lehman, T., Rainwater, K.A., Rajagopalan, S., Ridley, M., Tock, W.R., 2004. Distribution and Potential Sources of Perchlorate in the High Plains Region of Texas. Final Report to the Texas Commission on Environmental Quality). .

Kang, N., Jackson, W.A., Dasgupta, P.K., Anderson, T.A., 2008. Perchlorate production by ozone oxidation of chloride in aqueous and dry systems. Sci. Total Environ. 405, 301–309.

Munster, J.E., 2008. Nonpoint Sources of Nitrate and Perchlorate in Urban Land Use to Groundwater. PhD Thesis. Stony Book University, Suffolk County, NY, pp. 115.

Munster, J.E., Hanson, G.N., 2009. Perchlorate and ion chemistry of road runoff. Environ. Chem. 6, 28–35.

Munster, J., Hanson, G.N., Andrew Jackson, W., Rajagopalan, S., 2008. The fallout from fireworks: perchlorate in total deposition. Water Air Soil Pollut. 198, 149–153.

Murphy, D.M., Thomson, D.S., 2000. Halogen ions and NO^+ in the mass spectra of aerosols in the upper troposphere and lower stratosphere. Geophys. Res. Lett. 27, 3217–3220.

Paulinski, S., 2012. Structural, Hydrogeologic Framework and Textural Model of the Rialto-Colton basin and the Chino and North Riverside Area. Master of Science Thesis. Department of Geology, California State University, Sacramento, pp. 171.

Phillips, D.L., Gregg, J.W., 2001. Uncertainty in source partitioning using stable isotopes. Oecologia 127, 171–179.

Plummer, L.N., Böhlke, J.K., Doughten, M.W., 2006. Perchlorate in Pleistocene and Holocene groundwater in north-central New Mexico. Environ. Sci. Technol. 40, 1757–1763.

Poghosyan, A., Sturchio, N.C., Morrison, C.G., Beloso Jr., A.D., Guan, Y., Eiler, J.M., Jackson, W.A., Hatzinger, P.B., 2014. Perchlorate in the Great Lakes: isotopic composition and origin. Environ. Sci. Technol. 48, 11146–11153.

Rajagopalan, S., Anderson, T.A., Fahlquist, L., Rainwater, K.A., Ridley, M., Jackson, W.A., 2006. Widespread presence of naturally occurring perchlorate in high plains of Texas and New Mexico. *Environ. Sci. Technol.* 40, 3156–3162.

Rao, B., Anderson, T.A., Orris, G.J., Rainwater, K.A., Rajagopalan, S., Sandvig, R.M., Scanlon, B.R., Stonestrom, D.A., Walvoord, M.A., Jackson, W.A., 2007. Widespread natural perchlorate in unsaturated zones of the Southwest United States. Environ. Sci. Technol. 41, 4522–4528.

SAIC; Science Applications International Corporation, 2004. Final report: operational history 1941-1945 Rialto ammunition back-up storage point. Report prepared for the U.S army corps of engineers Los Angeles district. Online. http://www.waterboards. ca.gov/rwqcb8/water_issues/programs/perchlorate/docs/dod_report.pdf.

SARWQCB; Santa Ana Regional Water Quality Control Board, 2005. Proposed Groundwater Monitoring Program, Cleanup and Abatement Order (CAO) R8-2003-0013, to Mr. Peter Wulfman. Division Manager, Solid Waste Management Division, County of San Bernardino, Department of Public Works November 29.

Schilt, A.A., 1979. Perchloric Acid and Perchlorates. GFS Chemicals, Columbus, OH, pp. 3–4.

Sturchio, N.C., Beloso Jr., A.D., Heraty, L.J., Wheatcraft, S., Schumer, R., 2014. Isotopic tracing of perchlorate sources in groundwater from Pomona, California. Appl. Geochem. 43, 80–87.

Sturchio, N.C., Hoaglund III, J.R., Marroquin, R.J., Beloso Jr., A.D., Heraty, L.J., Bortz, S.E., Patterson, T.L., 2012a. Isotopic mapping of perchlorate plumes. Ground Water 50, 94–102.

Sturchio, N.C., Böhlke, J.K., Gu, B., Hatzinger, P.B., Jackson, W.A., 2012b. Isotopic tracing of perchlorate in the environment. In: Baskaran, M. (Ed.), Handbook of Environmental Isotope Geochemistry. Springer-Verlag, New York, pp. 437–452.

Sturchio, N.C., Caffee, M., Beloso-L, A.D., Heraty, J.K., Böhlke, P.B., Hatzinger, W.A., Jackson, B., Gu, J.M., Heikoop, Dale, M., 2009. Chlorine-36 as a tracer of perchlorate origin. Environ. Sci. Technol. 43, 6934–6938.

Sturchio, N.C., Beloso Jr., A.D., Heraty, L.J., LeClair, J., Rolfe, T., Manning, K.R., 2008. Isotopic evidence for agricultural perchlorate in groundwater of the Western Chino Basin, California. In: Sixth International Conference on Remediation of Chlorinated Solvents, Monterey, CA. 18-22 May.

Sturchio, N.C., Böhlke, J.K., Beloso Jr., A.D., Streger, S.H., Heraty, L., Hatzinger, P.B., 2007. Oxygen and chlorine isotopic fractionation during perchlorate biodegradation: laboratory results and implications for forensics and natural attenuation studies. Environ. Sci. Technol. 41, 2796–2802.

Sturchio, N.C., Böhlke, J.K., Gu, B., Horita, J., Brown, G.M., Beloso Jr., A., Patterson, L.J., Hatzinger, P.B., Jackson, W.A., Batista, J.R., 2006. Stable isotopic composition of chlorine and oxygen in synthetic and natural perchlorate. In: Gu, B., Coates, J.D. (Eds.), Perchlorate Environmental Occurrences, Interactions, and Treatment. Springer, New York, pp. 93–109.

Trumpolt, C., Crain, M., Cullison, G.D., Flanagan, S.J.P., Siegel, L., Lathrop, S., 2005. Perchlorate: sources, uses, and occurrences in the environment. Remediation, Winter 65–89.

Urbansky, E.T., Brown, S.K., Magnuson, M.L., Kelly, C.A., 2001a. Perchlorate levels in samples of sodium nitrate fertilizer derived from Chilean caliche. Environ. Pollut. 112, 299–302.

Urbansky, E.T., Collette, T.W., Robarge, W.P., Hall, W.L., Skillen, J.M., Kane, P.F., 2001b. Survey of Fertilizers and Related Materials for Perchlorate. US Environmental Protection Agency, pp. 33 EPA/600/R-01/047.

USDA (US Department of Agriculture), 2013. US census of agriculture. Online. http://www.agcensus.usda.gov.

USEPA, 2014. U.S. Environmental Protection agency, Pacific southwest region 9: Superfund. Rockets, fireworks, and flares. Website. Online. http://www.epa.gov/region9/rff.

Woolfenden, L., Kadhim, D., 1997. Geohydrology and water chemistry in the Rialto-Colton basin, san Bernardino county, California. US Geological Survey Water Resources Investigations Report 97–4012, 101.

Woolfenden, L.R., 2007. Aquifer susceptibility to perchlorate contamination in a highly urbanized basin. Dec. 2-7 In: In: Trefry, M.G. (Ed.), Securing Groundwater Quality in Urban and Industrial Environments. Proceedings of the International Association of Hydrologic Scientists, Groundwater Quality 2007 324. IAHS Publication, Fremantle, Western Australia, pp. 156 1,1 CD-ROM.